



Heriot-Watt University
Research Gateway

Effect of Ethylene Glycol, Ethanol and Methanol On PVCap-Induced Hydrate Crystal Growth Inhibition in Methane Systems

Citation for published version:

Mozaffar, H, Anderson, R & Tohidi Kalorazi, B 2014, 'Effect of Ethylene Glycol, Ethanol and Methanol On PVCap-Induced Hydrate Crystal Growth Inhibition in Methane Systems', Paper presented at 8th International Conference on Gas Hydrates 2014, Beijing, China, 28/07/14 - 1/08/14.

Link:

[Link to publication record in Heriot-Watt Research Portal](#)

Document Version:

Peer reviewed version

General rights

Copyright for the publications made accessible via Heriot-Watt Research Portal is retained by the author(s) and / or other copyright owners and it is a condition of accessing these publications that users recognise and abide by the legal requirements associated with these rights.

Take down policy

Heriot-Watt University has made every reasonable effort to ensure that the content in Heriot-Watt Research Portal complies with UK legislation. If you believe that the public display of this file breaches copyright please contact open.access@hw.ac.uk providing details, and we will remove access to the work immediately and investigate your claim.

EFFECT OF ETHYLENE GLYCOL, ETHANOL AND METHANOL ON PVCAP-INDUCED HYDRATE CRYSTAL GROWTH INHIBITION IN METHANE SYSTEMS

Houra Mozaffar^{1,2}, Ross Anderson^{1,2*}, and Bahman Tohidi^{1,2}

1. Centre for Gas Hydrate Research, Heriot-Watt University, Edinburgh, EH14 4AS,
Scotland, United Kingdom & 2. HYDRAFACT Ltd., Heriot-Watt University Research Park,
Edinburgh EH14 4AP, Scotland, United Kingdom

ABSTRACT

Methanol (MeOH), mono-ethylene-glycol (MEG) and increasingly ethanol (EtOH) are the most widely used thermodynamic inhibitors (THIs) for hydrate inhibition in hydrocarbon production operations. However, the use of thermodynamic inhibitors can have the disadvantages in that large quantities of inhibitor may be required, meaning large storage, regeneration and injection facilities which increase CAPEX/OPEX, in addition to environmental concerns. As a result, low dosage Kinetic Hydrate Inhibitors (KHIs) are seeing increasing use as a potential alternative for hydrate prevention, either partly or wholly replacing THIs. Combining KHIs with THIs offers a potential means to increase the subcooling to which KHIs can be used (THI acts as a 'top-up' inhibitor), while KHIs can be potentially used to reduce THI volumes. If the benefits of such combinations are to be realised, a better understanding of combined performance is required. Here, we report the results of experimental studies of combined KHI (PVCap, poly-n-vinylcaprolactam) – THI methane hydrate inhibition performance for MEG, MeOH and EtOH measured using a Crystal Growth Inhibition (CGI) method previously developed in this laboratory. Results show that neither MeOH nor EtOH act as full 'top-up' thermodynamic inhibitors for PVCap; KHI-induced CGI regions are consistently reduced to lower subcoolings as THI concentration is increased in both cases, although the negative effect is more pronounced with EtOH. In contrast, MEG was found to consistently act as a full 'top-up' thermodynamic inhibitor to PVCap; CGI regions being larger or equal to those for PVCap alone, and being present on top of the thermodynamic inhibition offered by MEG up to concentrations of 50 mass%. Furthermore, MEG has an increasingly synergistic effect on PVCap as the concentration is increased, reducing hydrate growth rates in CGI regions where growth does occur.

Keywords: gas hydrates, KHI, THI, MeOH, EtOH, MEG, crystal growth, inhibition

NOMENCLATURE

ΔT_{sub}	Subcooling [°C]
ΔP_{h}	Change in pressure due to hydrate formation [bar]
CIR	Complete (hydrate) Inhibition Region
CGI	Crystal Growth Inhibition
KHI	Kinetic Hydrate Inhibitor
PVCap	Poly-n-vinylcaprolactam
PVP	Poly-n-vinylpyrrolidone
RGR	Rapid (hydrate) Growth (rate) Region
SDR	Slow (abnormally, hydrate) Dissociation Region

SGR	Slow (hydrate) Growth (rate) Region
THI	Thermodynamic inhibitor
SG	Second Germination (KHI test method)
t_i	Hydrate nucleation induction time [hrs]

INTRODUCTION

While Thermodynamic Hydrate Inhibitors (THIs) such as methanol and MEG are widely used for hydrate prevention in the oil and gas industry, the large quantities of inhibitor often required can result in significant CAPEX/OPEX. As a result, recently, the use of Kinetic Hydrate Inhibitors

* Corresponding author: Phone: +44 (0)131 451 3798 Fax +44 (0)131 451 3127 E-mail: ross.anderson@pet.hw.ac.uk

(KHIs) has become increasingly popular over traditional thermodynamic inhibitors as an alternative, more cost effective technology [1,2,3]. Furthermore, for high subcooling operations, KHIs offer a potential means to reduce the amount of thermodynamic inhibitor required [4]. Likewise, thermodynamic hydrate inhibitors such as methanol and ethylene glycol can potentially be used as a 'top-up' inhibitor to KHIs, increasing the total inhibition offered. To fully exploit KHI-THI combinations however, it is important to understand their hydrate inhibition performance.

Research has shown that although methanol is an effective thermodynamic hydrate inhibitor, it can actually enhance the rate of hydrate formation when at low concentrations in water [5]. In addition, it has been found that, methanol (MeOH) has an unfavourable effect on the performance of PVCap; a well-known and one of the best performing KHI polymers [1]. The subcooling to hydrate formation decreases in linear proportion to the concentration of methanol, indicating that PVCap is less effective in the presence of methanol [6]. However, it has been found that the combination of thermodynamic inhibitors and kinetic inhibitors gives better results [7].

While the above findings are useful for understanding the influence of THIs on KHIs, techniques used in the mentioned investigations are limited to the onset of hydrate formation. In this work, our investigations have been undertaken using a new Crystal Growth Inhibition (CGI) technique, as developed by Anderson et al. [8]. Using this method has enabled us to avoid the problem of data stochasticity associated with nucleation / induction time measurements and produce very reliable/repeatable results. This information is beneficial for gaining a more comprehensive understanding of the effects of THIs on KHIs which is essential to be able to conclude how combinations perform in terms of hydrate inhibition. The new CGI method used in this study has increasingly become a popular method for KHI evaluation and is now being used by a number of companies in the oil and gas industry as a test protocol [9,10].

In addition to MeOH, ethanol (EtOH) is another alcohol which is seeing increasing use as a thermodynamic hydrate inhibitor due to its better environmental credentials. However, ethanol can

in fact form clathrate hydrates at conditions pertinent to offshore operations [11]. Hence, carefully evaluating the effect of this thermodynamic inhibitor on KHI performance is also crucial for understand the behaviour of the KHI-EtOH combinations.

Mono Ethylene Glycol (MEG) is one of the most widely employed thermodynamic hydrate inhibitors and is a commonly used carrier solvent / synergist chemical in KHI formulations. However, there is limited research on the performance of combinations of glycols and KHIs as hydrate inhibitors. In one study by Wu et al. (2006), the inhibition performance of mono-ethylene-glycol (MEG) and a kinetic hydrate inhibitor (VC-713) were tested individually and together. The study showed that the combination of MEG and the kinetic inhibitor had an overall better performance [7]. On the other hand, a study by Yousif, 1998 on the hydrate control process with MEG has shown that although ethylene glycol is known to suppress hydrates when added in adequate amounts to water, it tends to enhance the rate and amount of hydrate formed when present in small concentrations [5]. Taking both these studies into consideration, further investigations on hydrate formation and growth behaviour in the presence of MEG + KHI is required to better understand combined performance.

EXPERIMENTAL

Equipment and Materials

All the experiments were performed using constant volume methods, conducted on in-house (Hydrifact/ Heriot-Watt University) designed/built 280 ml volume high pressure (max 410 bar) stainless steel or titanium (salt compatible) autoclave cells, as illustrated in Figure 1. Cell temperature in these set is controlled by circulating coolant from a programmable cryostat, which can maintain the cell temperature to within 0.1 °C, through a jacket surrounding the cell. The inside temperature of the cell is determined by a platinum resistance thermometer (PRT, ± 0.1 °C) which is connected to a computer for direct acquisition. Cell pressure is measured by either strain gauge pressure transducer (± 0.4 bar) or precision Quartzdyne (± 0.07 bar) transducer; these being regularly calibrated against a dead weight tester. The pressure transducer is mounted directly on the cell and connected to the same data acquisition

unit as the temperature. This allows real time monitoring and recording of cell temperature and pressure throughout different temperature cycles.

To achieve a thermodynamic equilibrium quickly and create a state where all phases have an equal as possible ability to interact with each other, a stirrer with a magnetic motor was used to agitate the test fluid. Accordingly, to aid further mass transfer and maximise reaction rates, the impeller speed was normally set at ~750 rpm, giving good shearing/co-mingling of aqueous and gaseous phases. Cell aqueous liquid volume fraction was typically 0.80-0.85.

The KHI polymer used in tests was poly-n-vinylcaprolactam (PVCap) which was Luvicap-EG base polymer (average molecular weight / AMW = ~7000) supplied by BASF with the ethylene glycol solvent removed by vacuum oven drying. Methanol and ethanol used in experiments were supplied by Fisher Scientific with a purity of 99.5%. Also, the Mono-ethylene-glycol used was supplied from SIGMA ALDRICH with a purity of 99.5%. Ultra high purity grade methane gas (99.995% pure) supplied by BOC was used. Solutions were prepared using deionized water throughout the experimental work with aqueous PVCap solutions prepared gravimetrically.

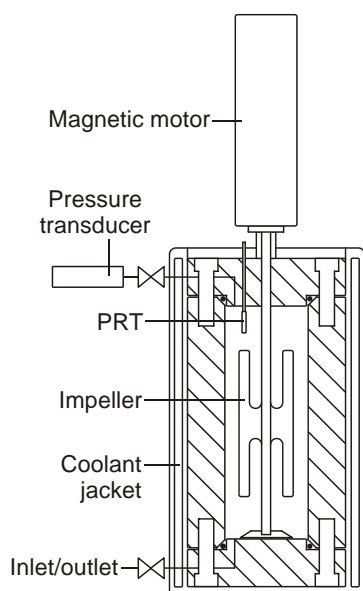


Figure 1 Schematic illustration of the 280 ml high pressure (max 410 bar) autoclave cells used in experiments.

In all experiments, the thermodynamic hydrate phase boundary was predicted using the HydraFLASH® 2.2 model from Hydrafact / Heriot-Watt University [12] or determined experimentally as appropriate by the isochoric step-heating method of Tohidi et al. [13].

As noted, the method used for KHI evaluation was the Crystal Growth Inhibition (CGI) technique as fully described by Anderson et al. [8]. In summary, in this method the system is initially cooled to high subcoolings from the hydrate phase boundary to induce hydrate formation. After this initial hydrate formation, the system is heated slowly outside the hydrate phase boundary leaving a small fraction of hydrate remaining (typically < 0.5% of water converted). Once only a small fraction of hydrate is left, temperature is again reduced but at a constant rate (e.g. 1.0 °C / hour) for detailed observation of growth rate changes as a function of subcooling. This is repeated a number of times for confirming repeatability. Finally, to confirm the extent of the complete inhibition and slow growth regions where appropriate, the system may be step-cooled with a small fraction of hydrate present [8].

Based on their studies, particularly the emerging close correlation between growth rates and exponential-type induction time trends, a simple logarithmic-type definition for CGI regions was defined by Anderson et al. [8] which is employed here (see Table 1).

Region	Hydrate Growth Rate Description	% Aqueous Phase Conversion Rate / hr
CIR	Completely inhibited	0.00
SGR(VS)	Very slow growth (VS)	≤ 0.1%
SGR(S)	Slow growth (S)	> 0.1% to ≤ 1.0%
SGR(M)	Moderate growth (M)	> 1.0% ≤ 10.0%
RGR	Rapid/fast	> 10.0% or as for no KHI present
SDR	Abnormally slow dissociation	One order of magnitude less than for no KHI

Table 1 CGI regions and respective growth rates. Rates are based on the assumption the system is non-static and well mixed.

RESULTS AND DISCUSSION

As noted, CGI experiments have been carried on MeOH-PVCap-Methane, EtOH-PVCap-water and MEG-PVCap-water systems at various THI concentrations. Results are discussed below.

Methane with PVCap and Methanol

Methane hydrate crystal growth patterns in the presence 0.50 mass% PVCap aqueous with a range of concentrations of methanol from 2.5 to 50 mass% (MeOH relative to water + PVCap) at pressures up to ~300 bar have been investigated.

Figure 2 shows example CGI method cooling / heating curves and CGI boundary data for methane-PVCap-methanol (2.5 mass% MeOH). Similar curves were obtained for all other methanol concentrations. The hydrate phase boundary is shown for comparison. As illustrated in this figure, CGI regions are clearly discernible from cooling curve data. Clearly the presence of 0.5 mass% PVCap induced the presence of characteristic ‘apparent’ complete inhibition (CIR – no detectable hydrate growth and/or hydrate dissociation), slow growth rate (SGR) and rapid growth/failure (RGR) regions. However, as will be explained, it is found that methanol overall had a detrimental effect on the subcooling extent of all regions at all concentrations tested compared to aqueous PVCap alone.

Previously in this lab, for methane-water-PVCap alone, it was found that the complete inhibition region extends to $\Delta T_{\text{sub}} = \sim -5.2$ °C. Also, it was found that ΔT_{sub} for the SGR(S) and RGR boundaries were ~ -7.2 °C and ~ -9.6 °C respectively [8]. However, data for the 5 different concentrations of methanol tested show that this alcohol has a consistently negative effect on the performance of PVCap; the extent of CGI region subcoolings reduce as methanol concentration increases. For example, the CIR region reduces from $\Delta T_{\text{sub}} = \sim -5.2$ °C to ~ -4.1 °C, ~ -2.4 °C, ~ -2.8 °C, ~ -2.9 °C and ~ -1.8 °C respectively at 2.5 mass%, 5.0 mass%, 10.0 mass%, 20.0 mass% and 50.0 mass% MeOH in the pressure range of 50 bar to 300 bar. Similarly, the extents of the SGR region / subcooling of the RGR boundary are also reduced to lower subcoolings as a function of increasing methanol concentration.

Figure 3 shows PVCap-induced inhibition regions as a function of aqueous (relative to water) methanol concentration. As evident from this figure, at low methanol concentrations (< 5 mass %), the SGR(S) region reduces rapidly as methanol is initially added to the system, before rising again slightly to a peak at ~5 mass% MeOH, beyond which it steadily reduces in subcooling extent again as methanol concentration rises. The reasons for this initial drop then recovery in performance are unknown, although it may be speculated that lower concentrations of methanol might be encouraging hydrate nucleation; methanol being known to form s-II hydrates at low temperatures [14].

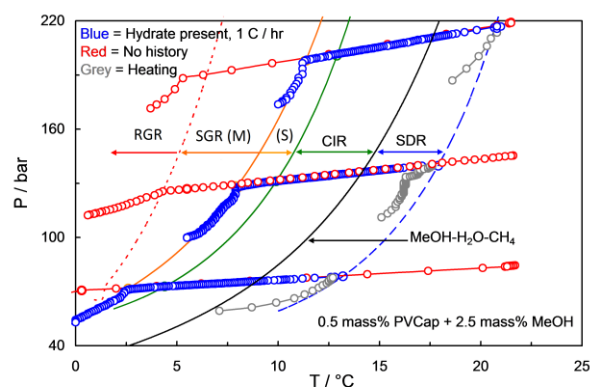


Figure 2 Example CGI cooling and heating curve data for 0.5 mass% PVCap / 2.5 mass% methanol aqueous with methane also showing CGI regions determined from changes in relative hydrate growth rates.

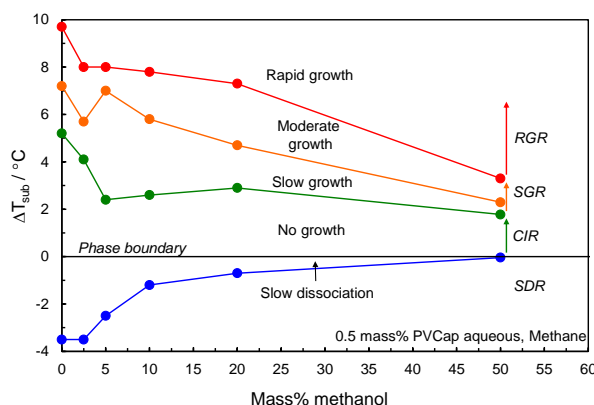


Figure 3 Average (50 to 300 bar) PVCap induced CGI regions for 0.5 mass% PVCap aqueous as a function of mass% methanol (relative to water + PVCap).

Finally, the slow dissociation region (SDR) consistently reduces to lower subcoolings as MeOH concentration increases, supporting CGI data in that MeOH is reducing PVCap effects on hydrate crystal growth and dissociation behaviour.

It should be noted that although the presence of MeOH has negative effect on PVCap performance, reducing the extent of all CGI regions, the combination of methanol and PVCap does still offer better inhibition by mass of inhibitor than methanol alone.

Methane with PVCap and Ethanol

Methane hydrate CGI region data have been generated for 0.5 mass% PVCap aqueous with 2.5, 11.4 and 50 mass% ethanol (relative to water + PVCap) at pressures up to ~150 bar.

Example CGI method cooling / heating curves and CGI boundary data are illustrated in Figure 4 for methane-PVCap-ethanol (2.5 mass% ethanol) system. Figure 5 shows PVCap-induced CGI regions as a function of aqueous (relative to water) ethanol concentration.

As shown in Figure 4, CGI regions are clearly distinguishable from cooling curve data. For all ethanol concentrations tested, in a similar case to methanol, ethanol overall had a detrimental effect on the subcooling extent of all CGI regions at all concentrations tested, although was overall less negative than methanol.

As mentioned and illustrated in Figure 4, results for 0.5 mass% PVCap and 2.5 mass% ethanol with methane show that ethanol has a generally negative effect on the performance of PVCap. It is apparent that while the SGR(S) and RGR region boundaries ($\Delta T_{sub} = \sim -7.5$ °C and ~ -9.3 °C respectively) remain at similar subcoolings to those for water-PVCap ($\Delta T_{sub} = \sim -7.3$ °C and ~ -9.6 °C respectively), the complete inhibition region reduces from $\Delta T_{sub} = \sim -5.2$ °C (for water-PVCap) to ~ -3.9 °C (for water-ethanol-PVCap). Therefore, although the presence of ethanol does not notably affect the overall extent of CGI regions, the CIR is reduced in subcooling extent which results in an overall negative ethanol effect.

As ethanol concentration increases, the negative effect on PVCap becomes more pronounced. For example, at 11.4 mass% ethanol (Figure 5), the complete inhibition region has been reduced to only $\Delta T_{sub} = \sim -1.2$ °C. Similarly, the SGR(S) and RGR boundaries are reduced to lower subcoolings of only $\Delta T_{sub} = \sim -5.1$ °C and -7.3 °C respectively.

Finally, tests with 50 mass% ethanol show that very high ethanol concentrations greatly reduce the performance of PVCap, so much so that the CIR has been completely lost, with only a small SGR region extending to $\Delta T_{sub} = \sim -1.6$ °C. This CGI reduction is reflected in there only being a very small SDR at higher ethanol concentrations ($\Delta T_{sub} = \sim +0.8$ °C for 11.4 mass% EtOH and $\Delta T_{sub} = \sim +0.3$ °C for 50 mass% EtOH), suggesting that polymer adsorption on crystal surfaces is growing weak due to the ethanol.

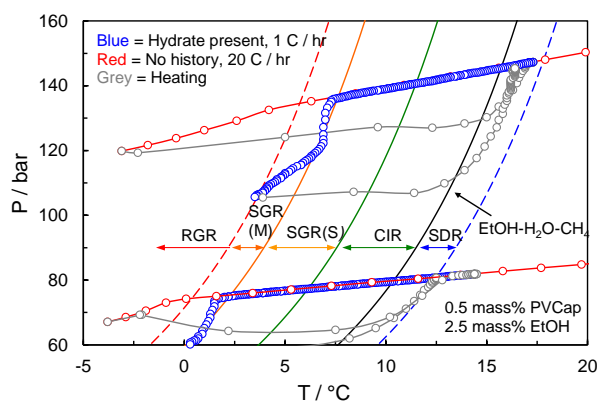


Figure 4 Example CGI test data for 0.5 mass% PVCap / 2.5 mass% ethanol aqueous with methane also showing determined CGI regions

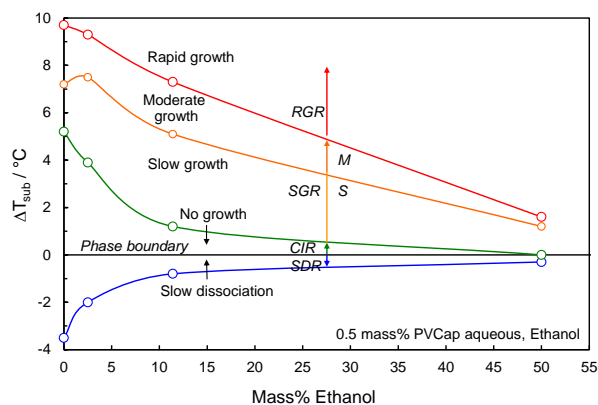


Figure 5 Average (40 to 120 bar) PVCap induced CGI regions for 0.5 mass% PVCap aqueous as a function of mass% ethanol (relative to water + PVCap).

To summarise, in a similar case to methanol, ethanol has a consistently negative effect on the performance of PVCap in methane systems; the extent of CGI region subcoolings reduced as ethanol concentration increased. As illustrated in Figure 5, the higher the EtOH concentration the smaller the CIR region becomes up to a point where it is completely lost at 50 mass% EtOH. Similarly, the SGR region is consistently reduced to lower subcoolings as a function of increasing ethanol concentration.

Finally, as for methanol, although the presence of EtOH has negative effect on PVCap performance and reduces the extent of CGI regions, the combination of ethanol and PVCap does still offer better inhibition by mass of inhibitor than ethanol alone.

Methane with PVCap and MEG

Methane hydrate CGI patterns in the presence of 1.0 mass% PVCap aqueous with a range of concentrations of MEG from 5.0 to 50.0 mass% (MEG relative to water + PVCap) at pressures up to ~300 bar have been investigated.

Example CGI method cooling / heating curves and CGI boundaries for methane–PVCap–MEG (5.0 mass% MEG) are illustrated in Figure 6. Figure 7 shows PVCap induced CGI regions as a function of aqueous (relative to water) MEG concentration.

As shown in Figures 6 and 7, in contrast to MeOH and EtOH, MEG generally acts as a ‘top-up’ inhibitor for PVCap for the concentrations tested; MEG generally shifts the PVCap-induced hydrate crystal growth inhibition regions by a subcooling equivalent to the degree of thermodynamic inhibition offered by that MEG aqueous fraction.

For example, as shown in Figure 7, the CIR remains constant at $\Delta T_{\text{sub}} = \sim -5.2 \text{ }^\circ\text{C}$ – which is the same as for water-PVCap alone – even up to concentrations as high as 50 mass% MEG. Likewise, the SGR(VS) region remains unchanged across the complete range of MEG concentrations tested. There is some variation in the SGR(S) and (M), although this is minimal and it is even larger in extent at 5.0 mass% MEG compared to PVCap alone.

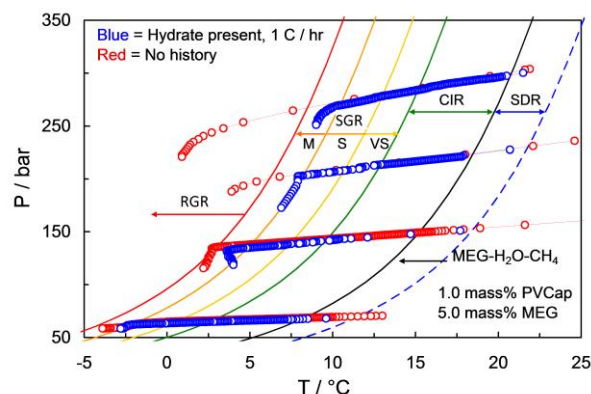


Figure 6 Example CGI cooling and heating curve data for 1.0 mass% PVCap / 5 mass% MEG aqueous with methane. Points are every 5 minutes.

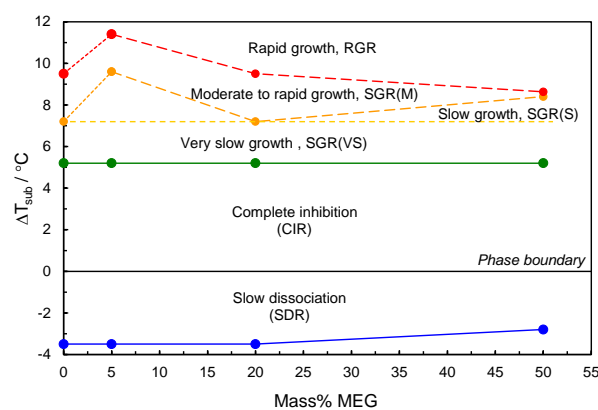


Figure 7 Average (50 to 300 bar) PVCap-induced CGI regions for 1.0 mass% PVCap aqueous as a function of mass% MEG (relative to water + PVCap).

A further observation in terms of the effect of MEG was that it greatly reduced growth rates, particularly in the SGR(VS). For example, in this region at 50 mass% MEG, growth rates were so slow that they were hardly detectable on the timescale of days. In that sense, the very slow growth region was almost an extension of the CIR and distinguishing of the two was difficult.

In conclusion, the presence of MEG has a very positive effect on PVCap performance and the combination of MEG + PVCap offers far better inhibition by mass/volume inhibitor than MEG alone. As MEG acts to all extents and purposes as a full ‘top-up’ inhibitor to PVCap to at least 50 mass%, it could in theory be used to extend the subcooling of KHIs and/or significantly reduce MEG thermodynamic inhibitor volumes.

CONCLUSIONS

In this work the effect of the thermodynamic hydrate inhibitors methanol, ethanol and MEG on the performance of the kinetic hydrate inhibitor polymer PVCap was investigated using the crystal growth inhibition (CGI) technique developed by Anderson et al. (2011).

Results for MeOH-PVCap-water and EtOH-PVCap-water showed that neither of these two alcohols acts as a 'top-up' thermodynamic inhibitor to PVCap; both have a clear negative impact on PVCap-induced CGI regions, although the combination of alcohol and PVCap does still offer better hydrate inhibition by mass of inhibitor than either of the alcohols alone. The reasons for this behaviour are unclear, although it could be related to the fact that both can enter hydrate cavities / form clathrate hydrates; methanol being capable of the latter at very low temperatures and ethanol at the conditions studied.

In contrast, data demonstrate that MEG generally acts as a full 'top-up' thermodynamic inhibitor for PVCap for the range of concentrations tested (up to 50 mass%). Furthermore, MEG can greatly reduce hydrate growth rates where growth can occur. The reasons why MEG, unlike methanol and ethanol, has a positive, synergist effect are unclear however and this would require further investigation.

ACKNOWLEDGEMENTS

This work was undertaken as part of a Joint Industry Project (JIP) at Heriot-Watt University, Scotland, UK, supported by Baker Hughes, Champion Technologies, Clariant Oil Services, DONG Energy, OMV, Petronas, Shell/NAM, Statoil and Total, whose support is gratefully acknowledged. Authors would like to thank Rod Burgass and Antonin Chapoy for their valuable contributions to the project, and Jim Allison for manufacture and maintenance of experimental equipment.

REFERENCES

[1] Kelland, M. A., 2006, *History of the development of low dosage hydrate inhibitors.*, Energy & Fuels 20(3): 825-847.
[2] Klomp, U., 2008, *The World of LDHI: From Conception to Development to Implementation*, Proceedings of the 6th

International Conference on Gas hydrates, Vancouver, Canada
[3] Sloan Jr, E. D. and C. Koh, 2007, *Clathrate Hydrates of Natural Gases*, Third Edition, CRC Press, New York
[4] Budd, D., Hurd, D., Pakulski, M., Schaffer, T. D., 2004, *Enhanced Hydrate Inhibition in Alberta Gas Field*, Proceedings of the SPE Annual Technical Conference and Exhibition, U.S.A, Texas, Houston
[5] Yousif, M.H., 1998, *Effect of Underinhibition with Methanol and Ethylene Glycol on the Hydrate-Control Process*, Proceedings of the Offshore Technology Conference, U.S.A, Texas, Houston, 184-189
[6] Sloan, E. D., Subramanian, S., Matthews, P. N., Lederhos, J. P., and Khokhar, A. A., 1998, *Quantifying Hydrate Formation and Kinetic Inhibition*, Industrial and Engineering Chemistry Research, 37, 3124-3132
[7] Wu, M., Wang, S., Lui, H., 2007, *A Study on Inhibitors for the Prevention of Hydrate Formation in Gas*, Journal of Natural Gas Chemistry, 16, 81-85
[8] Anderson, R., Mozaffar, H., Tohidi, B., 2011, *Development of a Crystal Growth Inhibition Based Method for the Evaluation of Kinetic Hydrate Inhibitors*, Proceedings of the 7th International Conference on Gas hydrates, Scotland, United Kingdom
[9] Glénat P, Bourg P, Bousqué M-L., 2013, *Selection of commercial Kinetic Hydrate Inhibitors using a new Crystal Growth Inhibition approach highlighting major differences between them*, SPE Middle East Oil and Gas Show, Manama, Bahrain, 10-13 March: SPE164258.
[10] Luna-Ortiz E, Healey M, Anderson R, Sørhaug E., 2014, *Assessing the performance of a kinetic hydrate inhibitor using a Crystal Hydrate Inhibition (CGI) method for a gas and gas-condensate system*, AiChE Spring Meeting - 2nd International Conference on Upstream Engineering and Flow Assurance, March 30th – April 3rd, New Orleans, USA.
[11] Anderson, R., Chapoy, A., Haghghi, H., and Tohidi, B., 2009, *Binary Ethanol–Methane Clathrate Hydrate Formation in the System CH₄-C₂H₅OH-H₂O: Phase Equilibria and Compositional Analyses*, Journal of Physical Chemistry C, 113, 12602–12607

- [12] http://www.hydrifact.com/software_hydrFLASH.html
- [13] Tohidi, B., Burgass, R.W., Danesh, A., Todd, A.C., and Østergaard, K.K., 2000, *Improving the Accuracy of Gas Hydrate Dissociation Point Measurements*, Annals of the New York Academy of Sciences, 912, 924-931
- [14] Shin, K., Udachin, K.A., Moudrakovski, I.L., Leek, D.M., Alavi, S., Ratcliffe, C.I., and Ripmeester, J.A., 2013, *Methanol Incorporation in Clathrate Hydrates and the Implications for Oil and Gas Pipeline Flow Assurance and Icy Planetary Bodies*, Proceedings of the National Academy of Sciences of the United States of America, 110(21): 8437-8442